Featured Letter

Intensifying internal electric field for efficient charge separation in different dimensions photocatalysts via in-situ crystallization

Kai Xu [a], Jiang Wu [a,*], Fengguo Tian [b,*], Qizhen Liu [c], Chenhao Qu [a], Weiguo Pan [a], Ping He [a], Humphrey Muzvidiwa [a], Zhen Zhang [a]

[a] College of Energy and Mechanical Engineering, Shanghai University of Electric Power, Shanghai 200090, China
[b] College of Environmental Science and Engineering, Donghua University, Shanghai 201620, China
[c] Shanghai Environment Monitoring Center, Shanghai 200030, China

ABSTRACT

A series of $BiOIO_3$ were prepared via in-situ crystallization method with different calcining temperatures. All samples were characterized by XRD, SEM, UV–vis, PL to explore the effect of internal electric field (IEF) among different dimensions. B-200 (calcinated under 200 °C) with the optimized IEF attained the most superior photocatalytic oxidation capacity in removing gas-phase Hg^0. Also, the formed 2D mixed 3D dimension changes the inter-atomic spacing to make the band bend upward, then moves the electrons and holes in the horizontally opposite direction. In combination with the above factors, the optimized IEF and dimension effectively intensify the separation of charge carriers and make the photocatalytic performance greatly improved.

1. Introduction

As is well-known, photo-generated electrons and holes play a decisive role in the photocatalytic process. Firstly, it takes several femtoseconds for catalysts to generate electron-hole pairs when accepting light [1]. Then a wide range from nanoseconds to some microseconds is spent to transfer charge carriers from the interior to the surface reaction area [2]. In contrast, the recombination of electrons and holes needs about several picoseconds. This means quite a lot of charge carriers tend to recombine rather than transfer to the surface reaction area [3], resulting in low separation efficiency and the poor photoactivity. Therefore, most of the existing methods have been adopted to boost the separation, for instance, metal and non-metallic doping [4], constructing defects [5], fabricating heterojunction [6], and so on. These methods have a certain effect on the separation of carriers. However, they can easily reduce the active sites and generate new recombination centers, which has the opposite effect on photoactivity. Thus, new strategies are required to promote separation urgently.

Internal electric field (IEF) is a potential self-motivation to effectively diffuse photogenerated carriers, which receives relatively less attention around the world. Photocatalysts with IEF, such as

$BiOIO_3$ [7], BiOCl [8] and $Bi_2O_2CO_3$ [9], have been reported as efficient photocatalysts in degradation of pollutants. Among them, $BiOIO_3$ has been the most promising photocatalysts due to its low toxicity and cost. The endogenetic force is induced by the polarization of the nonuniform charge distribution between disparate constituent lamellas, aurivillius-type $(Bi_2O_2)^{2+}$ layers and $(IO)^-$ pyramids [7], and enables separation of photoelectron-hole pairs instantly once generating [10].

In this work, we creatively used in-situ crystallization method with increasing calcining temperatures to fabricate different dimensions of $BiOIO_3$ in order to intensify the IEF. The properties in different dimensions of $BiOIO_3$ were then detected by the multiple characterization, and the removal efficiency of gas-phase Hg^0. It provided an easy method accompanied by changes in microstructure for separating photoelectrons and holes.

2. Materials and methods

2.1. Preparation of different dimensions of $BiOIO_3$

In-situ crystallization method was adopted to realize the converting from 2D to 3D of $BiOIO_3$. 8 mmol $Bi(NO_3)\cdot5H_2O$ and 8 mmol KIO_3 were dissolved into 150 ml deionized water to continuously stir for 30 min. Then, the mixture was put into an oven for 20 h, followed by grinding. Finally, the obtained powers of 0.5 g were calcined in the muffle furnace for 2 h with rate of 3 °C/min under

different calcination temperatures (180 °C, 200 °C, 250 °C, 300 °C, 350 °C, and 400 °C). Then the powers were slowly cooled down to room temperature naturally when heating was stopped. The as-prepared samples were named as B-180, B-200, B-250, B-300, B-350, and B-400 according to calcination temperatures respectively. The sample which was not calcined in the muffle furnace denoted as B-0.

2.2. Photocatalytic activity performance

A set of experimental system included the following three portions, simulated flue gas, photocatalytic reaction equipment, and on-line mercury analyzer, which was similar to our previous work [11]. The two mass flow meters (MFC, CS200 type) were utilized to control the flow rates of main and vice tubes, which were set as 0.2 L/min and 1 L/min. The main pipeline with 0.2 L/min passed through mercury generator, released stable gas-phase Hg^0 (55 μg/m^3) in 50 °C. Another channel transmitted carrier gas to mix with Hg^0, then entered into the on-line mercury analyzer (RA-915-M, Lumex, Russia) in order to calculate the concentration. Afterwards, the exhaust gas was filtered through activated carbon and KMnO$_4$ glass bottle (0.1 mol/L), and finally discharged into the atmosphere. During the experiment, 50 mg photocatalyst was carried out to evenly disperse on a quartz glass under the 9 W LED light with the filter (λ < 420 nm). The gas-phase Hg^0 concentration after the reaction was figured up with the following equation.

$$\eta_{Hg^0}(\%) = \left(1 - Hg^0_{out}/Hg^0_{in}\right) \times 100\% \tag{1}$$

where Hg^0_{in} and Hg^0_{out} represented Hg^0 concentration (μg/m^3) at the inlet and outlet of the system respectively.

3. Results and discussions

The crystal and phase structures were checked by X-ray diffraction shown in Fig. 1a. The location of diffraction peaks of all seven samples conforms to Inorganic Crystal Structure Database ICSD # 262019 (space group: Pca21; a = 5.6584(4), b = 11.0386(8), c = 5.7476(4) Å)[12] perfectly. The (1 2 1) peak enhances regularly attributed to increasing calcination temperatures. It indicates that a certain heating temperature does not make the sample deterioration, but can change the microstructure and advance the
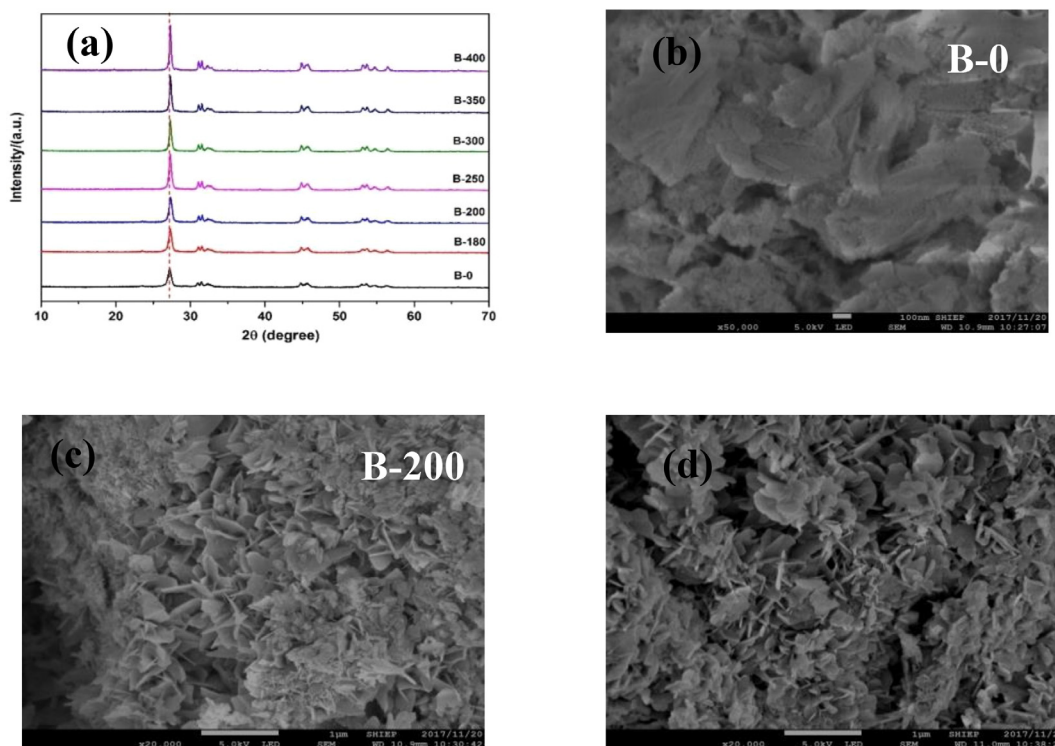

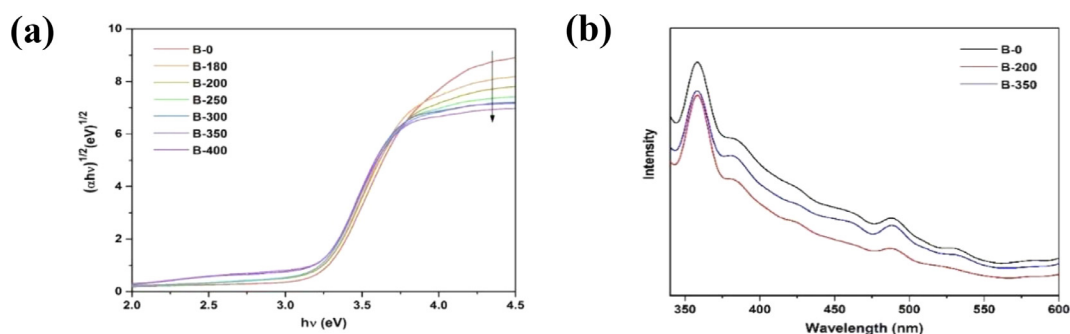**Fig. 1.** (a) XRD patterns of prepared samples; SEM images of (b) B-0, (c) B-200, (d) B-350.

Fig. 2. (a) UV–vis DRS spectra of as-prepared samples; (b) PL analysis of B-0, B-200, B-350.